

# EVALUATION OF A PERSONAL AND ENVIRONMENTAL DOSEMETER BASED ON CR-39 TRACK DETECTORS IN QUASI-MONOENERGETIC NEUTRON FIELDS

M. Caresana<sup>1</sup>, M. Ferrarini<sup>2,\*</sup>, A. Parravicini<sup>3</sup> and A. Sashala Naik<sup>1,3</sup>

<sup>1</sup>Politecnico di Milano, CESNEF, Dipartimento di Energia, via Ponzio 34/3, 20133 Milano, Italy

<sup>2</sup>Fondazione CNAO, strada privata Campeggi 53, 27100 Pavia, Italy

<sup>3</sup>Mi.am srl, via De Amicis 5, 29029 Fabiano di Rivergaro (PC), Italy

\*Corresponding author: michele.ferrarini@polimi.it

Solid-state nuclear track detectors (SSNTDs) can be successfully used to measure particle linear energy transfer (LET) by measuring the track image parameters<sup>(1, 2)</sup>. For practical applications, the LET can be used to derive a good approximation of the ambient dose equivalent and the personal dose equivalent<sup>(2)</sup>. The detector, meant for neutron dosimetry, is realised by coupling the CR-39 SSNTD, primarily made of polyallyl diglycol carbonate (PADC) to a PMMA [composition (C<sub>5</sub>O<sub>2</sub>H<sub>8</sub>)<sub>n</sub>] radiator. The neutron interaction in PMMA provides recoil proton via (n,p) elastic scattering. This channel of charged particle production dominates up to a neutron energy of around 7–8 MeV. For higher neutron energies, elastic and inelastic scattering cross section of oxygen and carbon becomes important. The effect on the passive detectors is that tracks are not only produced by recoil protons but by heavier charged secondary particles. The exact evaluation of the secondary particle energy distribution is out of the scope of the present paper.

## THEORY

The latent damage produced by the charged hadrons in the track detector can be enhanced via chemical etching. The key quantities describing the etching process are  $V_b$  and  $V_t$ , respectively, the bulk and track etch rates. From a qualitative point of view,  $V_t$  measures the ‘amount of damages’ produced at the surface of the track detector by the impinging particle and is proportional to the particle LET.  $V_t$  is proportional to the particle impinging energy and increases along the track according to the increase in LET with a ‘Bragg peak-like’ shape. On the other hand,  $V_b$  can be considered constant.

The  $V_t$  vs. LET proportionality permits to write the following equation:

$$\overline{\text{LET}} = f(V) \quad (1)$$

where  $V$  is the ratio  $V_t$  to  $V_b$ , considering the average  $V_t$  value along the etching duration. The analytical expression of the function  $f(V)$  used in this work is described in the work of Caresana *et al.*<sup>(2)</sup>. It is worth noticing that the LET calculated using Equation (1) is an average LET because it is calculated using an estimate of  $V_t$  measured on the track.

The  $V$  ratio is obtained by measuring the major and minor axes of the track opening<sup>(3)</sup> (see Figure 2). In this way, the impinging angle of the particle can be determined as well. The impinging angle is measured to the normal to the detector surface.

The measurement of the average LET and impinging angle of the particles are necessary to evaluate the energy deposited in the track detector by the secondary particles, and consequently calculate the dose equivalent (mSv) in the CR-39 detector by using the following equation.

$$H_{\text{cr}} = \frac{1}{\rho} \times 1.602 \times 10^{-6} \cdot \sum_{i=1}^n \frac{\overline{\text{LET}}_i}{\cos \theta_i Q(\overline{\text{LET}}_i)} \quad (2)$$

where

$\overline{\text{LET}}_i$  is the average LET of the  $i$ th track expressed in keV  $\mu\text{m}^{-1}$ ,  $Q(\overline{\text{LET}}_i)$  the corresponding ICRP quality factor,  $\theta_i$  the particle impinging angle with respect to the normal to the detector surface,  $n$  the number of tracks detected per square  $\text{cm}^2$  and  $\rho$  is the polymer density expressed in  $\text{g cm}^{-3}$ . The numerical

factor is a key element to obtain the dose equivalent expressed in mSv.

Equation (2) represents an approximation of  $H$  for the following reasons:

- The secondary particles impinging with an angle above the limit angle are not detected.
- Recoil protons with energies higher than  $\sim 10$  MeV are not detected.
- The ICRP quality factors are defined in water but not in CR-39.

Some tracks are produced due to secondary particles generated from (n,p) elastic scattering of primary neutrons on the hydrogen atoms inside the CR-39 detector or itself.

For these reasons the quantity calculated using Equation (2), named  $H_{cr}$  has to be regarded as a response function of the track detector representing the best estimation of the equivalent dose made using track detectors, and for the geometry of the detector it can be successfully used as an estimate of  $H^*(10)$  and  $H_p(10)$ . Further description of this type of analysis can be found in the work of Caresana *et al.*<sup>(2)</sup>.

## MATERIALS AND METHODS

The detection system consists of a CR-39 SSNTD covered with 1 cm of a PMMA radiator. Tracks in the PADC detector are produced either by recoil protons or heavy charged particles produced by neutron interactions in the PMMA radiator and in the CR-39 itself.

The dosimeters were exposed to neutron energies ranging from 0.565 to 100 MeV.

At the PTB in Braunschweig, the irradiations were performed without phantom at the following ISO reference monoenergetic neutron beams listed in Table 1.

The irradiations in high-energy neutrons were performed at the iThemba Laboratory (iTTL) for Accelerator-Based Sciences. The calibration facility can produce quasi-monoenergetic neutrons ranging from 25 to 200 MeV through  ${}^7\text{Li}(p,n){}^7\text{Be}$  reaction on a thick Li target (6 mm)<sup>(4)</sup>. The neutron beam is 10 cm  $\times$  10 cm wide and the metrological

characterisation of the beam in terms of dosimetry and spectrometry was performed by the PTB<sup>(5)</sup>.

The detectors were irradiated both at  $0^\circ$  and  $16^\circ$  using 66- and 100-MeV quasi-monoenergetic neutrons. In Figure 1 the neutron spectra in the 100-MeV case is shown. In principle, the irradiation at  $16^\circ$  should be used to subtract the portion of the neutron spectrum out of the main peak in order to obtain the detector response at an ideal monoenergetic peak. Such an analysis was not performed in this work but the irradiation were simply considered as reference irradiation with a given neutron energy distribution with a predominant high-energy component.

The CR-39 track detectors used in this work are produced by InterCast<sup>®</sup> are  $25 \times 25 \text{ mm}^2$  in surface area, 1.5 mm thickness and have a density of  $1.31 \text{ g cm}^{-3}$ . After exposition, the detectors were chemically etched in a 6.25-mol aqueous NaOH solution at  $98^\circ\text{C}$  for 90 min to reveal the tracks formed at the surface of the

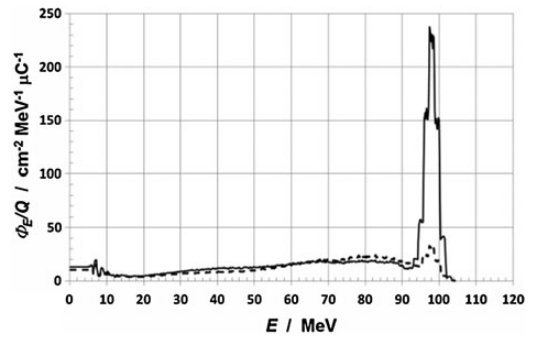


Figure 1. Neutron energy distributions of fluence for incident proton energy of 100 MeV at  $0^\circ$  (solid) and  $16^\circ$  (dashed).

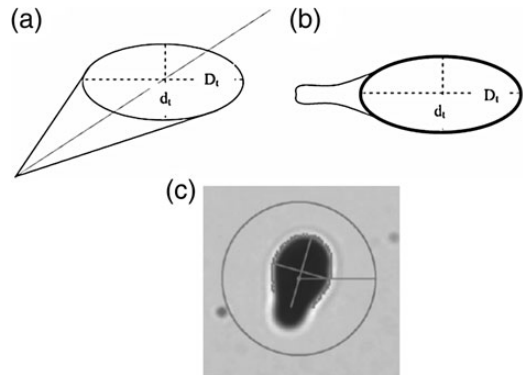


Figure 2. (a) Example of the conical shape of the track. (b) Top view of the track as seen by the microscope showing the major axis  $D$  and the minor axis  $d$ . (c) Image analysis of a real track by the Politrack<sup>TM</sup> software.

Table 1. Neutron beams used for irradiations at PTB.

Reaction	$\langle E_n \rangle$ (MeV)	$d\phi/dt$ ( $\text{cm}^{-2}\cdot\text{s}^{-1}$ )	$dH^*(10)/dt$ ( $\text{mSv}\cdot\text{h}^{-1}$ )
$\text{Li}(p,n){}^7\text{Be}$	0.565	$1.2 \times 10^3$	1.5
${}^2\text{H}(d,n){}^3\text{He}$	8.0	$1.9 \times 10^4$	27.5
${}^3\text{H}(d,n){}^4\text{He}$	14.8	$1.3 \times 10^4$	24.2
${}^3\text{H}(d,n){}^4\text{He}$	19.0	$1.3 \times 10^4$	1.8

CR-39 plastic. Using the fission fragment technique<sup>(2)</sup>, the bulk attack velocity  $V_b$  was determined to be of  $10 \pm 0.2 \mu\text{m}\cdot\text{h}^{-1}$ . The detectors were then analysed using the Politrack<sup>TM</sup> commercial reader developed at Politecnico di Milano and Mi.am srl.

At the surface of the detector, the entrances of the cone-shaped tracks have an elliptical shape defined by the major and minor axes, respectively,  $D$  and  $d$  as illustrated by Figure 2. The figure shows how the image analysis software of the Politrack<sup>TM</sup> instrument does an elliptical fit on the images taken of the detector to measure the axes  $D$  and  $d$  for each track<sup>(2)</sup>. From the measurement of the axes the analysis described in the section Materials and methods was carried out.

## RESULTS AND DISCUSSION

The LET distributions for each irradiated detectors are calculated using the theory developed in the section Materials and methods. Figures 3 and 4 show an example of the average LET (named  $\text{LET}_{\text{nc}}^{(2)}$ ) distribution measured for detectors irradiated at 8 MeV (PTB) and 100 MeV (iTLL) fast neutrons, respectively.

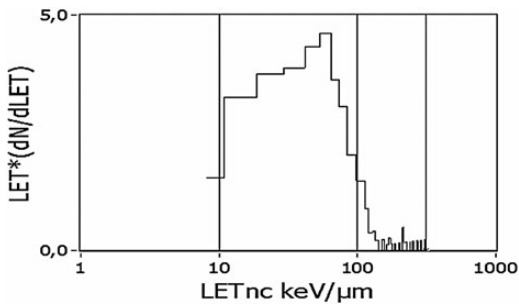


Figure 3.  $\text{LET}_{\text{nc}}$  distribution measured in the 8-MeV neutron beam at PTB.

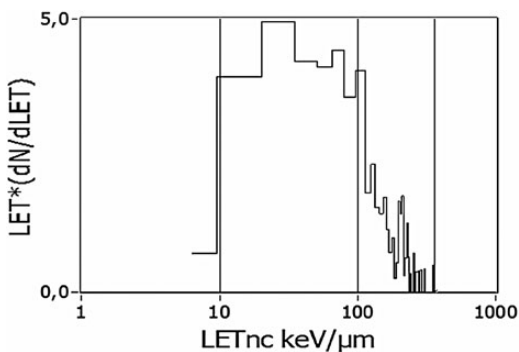


Figure 4.  $\text{LET}_{\text{nc}}$  distribution measured at  $0^\circ$  in the 100-MeV neutron beam at iTLL.

The average LET produced by recoil protons has a maximum of around  $100 \text{ keV } \mu\text{m}^{-1}$ . The signal at higher LET value is due to secondary particles other than protons ( $^3\text{He}$ ,  $^4\text{He}$ , or recoil carbon and oxygen). It is thus possible to split the measured  $H_{\text{cr}}$  in two contributions, below and above  $100 \text{ keV } \mu\text{m}^{-1}$ .

In Figure 3, the measured  $H_{\text{cr}}$  from particles having an  $\text{LET} < 100 \text{ keV } \mu\text{m}^{-1}$  is 1.58 mSv and for an  $\text{LET} > 100 \text{ keV } \mu\text{m}^{-1}$  is 0.2 mSv. The total  $H_{\text{cr}}$  is 1.78 mSv with a distribution ratio of 0.12. This is an indication that most of the equivalent dose is due to recoil protons.

In Figure 4, measured  $H_{\text{cr}}$  for particles having an  $\text{LET} < 100 \text{ keV } \mu\text{m}^{-1}$  is 0.68 mSv and for an  $\text{LET} > 100 \text{ keV } \mu\text{m}^{-1}$  is 0.75 mSv. The total  $H_{\text{cr}}$  is 1.43 mSv with a distribution ratio ( $H_{\text{cr}} > 100 \text{ keV } \mu\text{m}^{-1} / H_{\text{cr}} < 100 \text{ keV } \mu\text{m}^{-1}$ ) of 1.1.

A particular attention has to be devoted to the background detectors. Figure 5 illustrates the LET distribution measured on a detector stored at low temperature, for  $\sim 4$  y, and sealed in a radon-proof material to avoid radon contamination. The LET analysis shows a total  $H_{\text{cr}}$  of 0.25 mSv with a distribution ratio of 2.6 ( $H_{\text{cr}} < 100 \text{ keV } \mu\text{m}^{-1} = 0.07$ ;  $H_{\text{cr}} > 100 \text{ keV } \mu\text{m}^{-1} = 0.18$ ). This is a clear indication that most of the background signal is due to the production of secondary particles from high-energy cosmic rays.

The low LET component gives a lower contribution even if the total number of tracks in this region is higher. This is because the relative weight of low LET particles in Equation (2) is lower. Moreover, most of the signal in terms of track number is in the LET bin of around  $10 \text{ keV } \mu\text{m}^{-1}$  and the total  $H_{\text{cr}}$  in this region is estimated to be a few  $\mu\text{Sv}$ . It is important to notice that some plastic defects that could be mistaken as tracks are concentrated mainly in this LET region. Eventually, the response function calculated after Equation (2) has the merit of greatly

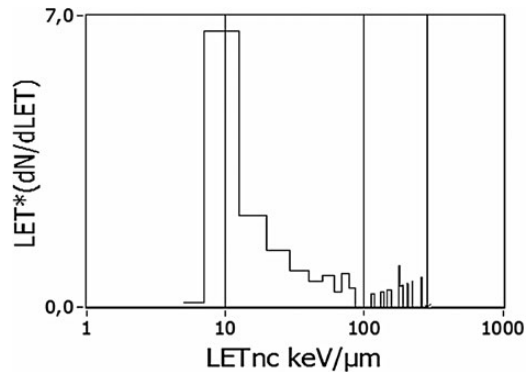


Figure 5. Background radiation from cosmic rays induced secondary particles measured in CR-39.

**Table 2. Detector response measured for the different neutron beam energies ranging from 0.5 MeV to 100 MeV at the PTB and iTL particle accelerators.**

Beam	Reference $H^*(10)$ (mSv)	Measured $H_{cr}$ (mSv)	Response
PTB 565 KeV	3.67	1.79	0.49
PTB 8 MeV	4.90	1.75	0.36
PTB 14 MeV	6.90	3.49	0.51
PTB 19 MeV	2.90	1.84	0.64
iTL 66 MeV 0°	4.44	2.38	0.54
iTL 66 MeV 16°	3.20	1.72	0.54
iTL 100 MeV 0°	2.36	1.52	0.64
iTL 100 MeV 16°	2.83	1.75	0.62

**Table 3. Measured  $H_{cr}$  in different detectors exposed at 0° in the 66-MeV neutron beam at iTL.**

Detector	CHI <sup>2</sup>	$H_{cr}$ (mSv)		
1608	1.03	2.25	Mean $H_{cr}$ (mSv)	2.38
1614	1.06	2.29	St. dev.	0.23
1640	1.11	2.55	St. dev. %	9.7
1646	0.91	2.21	Ref. $H^*(10)$ mSv	4.44
1654	1.06	2.19	Response	0.54
1675	0.99	2.42		
1693	0.92	2.25		
1694	1.05	2.87		

underestimating the contribution of plastic defects mimicking tracks.

The detector signal calculated using Equation (2) shows that the response of the detection system varies slightly around a value of 0.54 with an uncertainty of ~10 %, independently on the neutron energy as illustrated in Table 2.

This is a remarkable result because it demonstrates that the detector can work in an ‘REM-counter-like’ way.

To check the repeatability of the measurements done throughout the experimental campaign, the CHI<sup>2</sup> test was used for each exposition. Table 3 reports the results for the measurement of eight detectors simultaneously exposed in the 66-MeV neutrons at 0° with respect to the incident beam at the iTL. The CHI<sup>2</sup> test is the statistical check to control that the tracks follow a Poisson distribution on the detector surface with a theoretically expected value of 1. Each one of the eight detectors falls in the

acceptable range of  $1 \pm 0.12$ , confirming a good distribution of the tracks on the detector surface.

As shown in Table 3 the standard deviation of the measurements for this beam energy is around 10 % and corresponds to the value found for the remaining irradiations performed, thus giving a solid argument for the repeatability of the measurements done with the passive dosimetry system.

## CONCLUSION

Using the method described in this paper, the response of the PADC detectors, coupled with plastic converters proved to be almost independent of the neutron energy, in a wide energy range (0.565–100 MeV). This is particularly interesting for personal and environmental dosimetry applications, since this neutron energy range is wide enough for these detectors to be successfully used in many practical situations, for example, isotopic sources and in accelerator environment.

Moreover, they can be used to estimate the ambient dose equivalent component due to high-LET particles in mixed radiation fields. For many applications, this component is a good approximation of the ambient dose equivalent, and can be also used to estimate the personal dose equivalent.

## FUNDING

This research has been partially supported by a Marie Curie Early Initial Training Network Fellowship of the European Community’s Seventh Framework Programme under contract number (PITN-GA-2011-289198-ARDENT).

## REFERENCES

1. Nikezic, D. and Yu, N. K. *Formation and growth of tracks in nuclear track materials*. Mater. Sci. Eng. Rev. **46**, 51–123 (2004).
2. Caresana, M. *et al.* *Determination of LET in PADC detectors through the measurement of track parameters*. Nucl Instrum Methods A, **683**, 8–15 (2012).
3. Caresana, M. *et al.* *Study of a radiator degrader CR39 based neutron spectrometer*. Nucl. Instrum. Methods A **620**, 368–374 (2010).
4. Mosconi, M. *et al.* *Characterisation of the high-energy neutron beam at iThemba LABS*. Radiat. Meas. **45**, 1342–1345 (2010).
5. Harano, H. *et al.* *Quasi-monoenergetic high-energy neutron standards above 20 MeV*. Metrologia **48**, S292–S303 (2011).